1,2,4-Triazole and Its Derivatives as Corrosion Inhibitors for Aluminum Brass (HAl77-2) in 3.5 *wt.*% NaCl Solution

Di ZHU, Hong JU *, Hanzhi LI, Xupeng JIA

School of Materials Science and Engineering, China University of Petroleum (East China), 66 Changjiang west Road, Huangdao District, Qingdao, China, 266580

http://doi.org/10.5755/j02.ms.38849

Received 18 September 2024; accepted 9 December 2024

In this work, the 1,2,4-triazole and its derivatives were used as target corrosion inhibitors, the corrosion inhibition of 1,2,4-triazole (TAZ), 3-amino-1,2,4-triazole (ATA) and 3,5-diamino-1,2,4-triazole (DAT) in 3.5 wt.% NaCl solutions for aluminum brass (HAl77-2) are reported. The inhibition properties and mechanism were investigated by weight loss tests, electrochemical tests (electrochemical impedance spectroscopy and linear polarization resistance tests), surface characteristic analysis (scanning electron microscopy (SEM) and energy-dispersive X-ray spectroscopy (EDS) tests), and quantum chemistry calculations. The results showed that TAZ, ATA, and DAT effectively inhibited the corrosion of HAl77-2. The maximum inhibition efficiencies of the three corrosion inhibitors were 84.4 %, 86.4 %, and 87.1 %, respectively. The adsorption processes followed the Langmuir adsorption isotherm model and were of mixed type, i.e., both physisorption and chemisorption. SEM and EDS tests confirmed the effective adsorption of the TAZ, ATA, and DAT on the HAl77-2 surface. The results of quantum chemistry calculations were consistent with the electrochemical test results.

Keywords: 1,2,4-triazole, corrosion inhibitor, aluminum brass, electrochemical test, quantum chemistry calculation.

1. INTRODUCTION

Copper and copper-based alloys are used in various fields because of their high corrosion resistance [1 – 3]. However, in seawater media, copper and its alloys are subject to severe corrosion due to the harsh environment. HAl77-2, as an aluminum brass, has good corrosion resistance and is widely used as a heat-transfer tube material [4, 5]. As one of the core components of low-temperature multi-effect desalination (LT-MED) devices, aluminum brass (HAl77-2) heat-transfer tubes are susceptible to erosion by chloride ions after long periods of operation, which shortens the service life and causes safety hazards and economic losses. Therefore, taking reasonable protective measures is of great significance to extend the mission lives of the devices and reduce the cost of industrial water desalination.

The use of corrosion inhibitors is one of the main methods to control the corrosion of metals [6]. Corrosion inhibitors are widely used in petroleum, chemical, machinery, and other fields because of their advantages, such as low costs, low required dosages, and significant effects [7]. Recently, the awareness of ecological protection has gradually increased, and the development of eco-friendly organic corrosion inhibitors has become a research hotspot [8, 9]. The molecular structures of organic corrosion inhibitors usually contain heteroatoms (e.g., N, O, S, and P) or aromatic rings, which enable them to interact with metal surfaces [9 – 11]. Organic molecules form a protective film that prevents the entry of corrosive ions and thus acts as a corrosion inhibitor.

It is well known that azoles have a good affinity with copper and exert corrosion inhibition by forming protective films. Benzotriazole and its derivatives have shown good corrosion inhibition performances as well-established corrosion inhibitors for copper-based materials [12, 13]. However, their toxicity has limited their application in different environments [14, 15]. In comparison, 1,2,4-triazole and its derivatives are less toxic and have better degradability, exhibiting good inhibitory effects as effective corrosion inhibitors for pure copper in different media environments [15, 16]. However, few studies have been reported on the corrosion inhibition of aluminum brass in neutral sodium chloride media. Then, in this study, 1,2,4-triazole (TAZ), 3-amino-1,2,4-triazole (ATA), and 3,5-diamino-1,2,4-triazole (DAT) were screened as target corrosion inhibitors.

2. EXPERIMENTAL

2.1. Pre-experiment preparation

The studied metal was HAl77-2 aluminum brass. Its composition is shown in Table 1. The samples used for electrochemical tests were 1 cm × 1 cm × 0.5 cm in size and were sealed with epoxy resin after connecting the copper wires. The exposure area was 1 cm^2. The samples were ground step by step with silicon carbon papers (400, 800, 1200 and 1500 grits) before the experiments, then they were cleaned with pure water and anhydrous ethanol, dried and prepared for use.

* Corresponding author: H. Ju
E-mail: *juhong@upc.edu.cn*

Table 1. Composition of aluminum brass (HAl77-2)

Elements, wt.%	Cu	Al	Pb	Fe	Sb	As	P	Zn
	76	1.9	0.03	0.05	0.04	0.06	0.02	Rest

The tested solution was a 3.5 wt.% NaCl solution, prepared with sodium chloride (analytical grade) and deionized water.

As shown in Fig. 1, the tested corrosion inhibitors were 1,2,4-triazole (purity: 99 %), 3-amino-1,2,4-triazole (purity: 96 %), and 3,5-diamino-1,2,4-triazole (purity: 98 %), purchased from Shanghai Macklin Biochemical Co., Ltd.

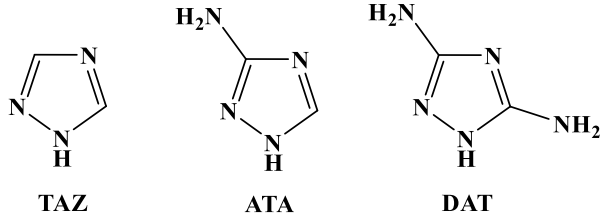

Fig. 1. Chemical structures of TAZ, ATA and DAT

2.2. Weight loss tests

The samples (5.0 cm × 2.5 cm × 0.5 cm) were sanded step by step with silicon carbon papers (400, 800, 1200 and 1500 grits) before the experiments, rinsed with pure water, degreased with acetone, ultrasonically cleaned with anhydrous ethanol, blown dry and placed in a desiccator, weighed on an analytical balance after 24 hours to be used for spare parts, and then immersed in 3.5 wt.% NaCl solution containing different concentrations (0 mmol/L, 1 mmol/L, 1.5 mmol/L, 2 mmol/L, 2.5 mmol/L, 3 mmol/L) of corrosion inhibitors for 7 days at 303 K. After 7 days, the samples were wiped with a fine brush, dilute hydrochloric acid was prepared to remove the surface corrosion products, cleaned with pure water, degreased with acetone, ultrasonically cleaned with anhydrous ethanol, blown dry and placed in a desiccator, weighed again after 24 hours, and the weight loss before and after immersion of the samples was observed and recorded. To reduce the experimental error, three parallel groups of samples were set up under each corrosion inhibitor concentration, and the average value was taken.

2.3. Electrochemical tests

Electrochemical tests were performed using a CS310M system and a conventional three-electrode system with HAl77-2 aluminum brass as the working electrode, a saturated calomel electrode (SCE) as the reference electrode, and a platinum sheet as the counter electrode. Electrochemical impedance spectroscopy (EIS) and linear polarization resistance (LPR) curves were tested after the open circuit potential was stabilized (the potential fluctuation was less than 3mV within 5 minutes). The EIS test frequency range was 105 Hz ~ 102 Hz, and the amplitude was 10 mV. For the LPR tests, the potential range was Eocp ± 10 mV, and the scan rate was 0.1667 mV/s.

2.4. Surface characteristic analysis

HAl77-2 samples were sanded and polished, then immersed in 3.5 wt.% NaCl solutions free of and containing inhibitors for 72 h at 30 °C. The concentration of the three corrosion inhibitors was 3 mmol/L. The surface morphologies were observed via SEM (JEOL SM-14041SNS2). The working voltage was 15 kV. The elemental compositions of the sample surfaces were determined via EDS (OXFORD X-Max50).

2.5. Calculation details

Quantum chemistry calculations were performed using GaussView 6.0 and Gaussian09W. The molecular structures of the three corrosion inhibitors were optimized at the B3LYP/6-311+G (d, p) level based on density functional theory (DFT). Based on the calculations, several important parameters were obtained.

3. RESULTS AND DISCUSSION

3.1. Weight loss tests

The weight loss tests were performed as described in subchapter 2.2. The corrosion inhibition efficiency was calculated by the following equation:

$$IE(\%) = \frac{W_0 - W}{W_0} \times 100, \quad (1)$$

where W_0 and W are the weight loss per unit area in mg/cm^2 without and with the presence of the corrosion inhibitor, respectively.

As can be seen in Table 2, the corrosion of HAl77-2 aluminum brass in 3.5 wt.% NaCl solution can be effectively inhibited by adding different concentrations of TAZ, ATA, and DAT, respectively.

Table 2. Weight loss results after adding various concentrations of three inhibitors

Inhibitors	C, mmol/L	ΔW, mg/cm^2	IE, %
	Blank	0.3262	–
TAZ	1.0	0.1108	66.0
	1.5	0.0954	70.8
	2.0	0.0862	73.6
	2.5	0.0769	76.4
	3.0	0.0677	79.2
ATA	1.0	0.0667	79.6
	1.5	0.0625	80.8
	2.0	0.0554	83.0
	2.5	0.0544	83.3
	3.0	0.0492	84.9
DAT	1.0	0.0646	80.2
	1.5	0.0585	82.1
	2.0	0.0516	84.2
	2.5	0.0451	86.2
	3.0	0.0400	87.7

As the concentrations of corrosion inhibitors increased, the coverage of corrosion inhibitors on the surface of aluminum brass gradually increased, thereby making the weight loss per unit area gradually reduced, and the samples' surfaces were well protected. The weight loss per unit area reaches the minimum value when the concentration of

corrosion inhibitor was 3 mmol/L, and the order of the highest corrosion inhibition efficiency was DAT(87.7 %) > ATA (84.9 %) > TAZ (79.2 %). The higher the concentrations of the three corrosion inhibitors, the more significant the corrosion inhibition effect on HAl77-2 aluminum brass.

3.2. Electrochemical impedance spectroscopy (EIS) tests

Fig. 2 and Fig. 3 show the Nyquist and Bode plots containing different concentrations of TAZ, ATA, and DAT at 30 °C.

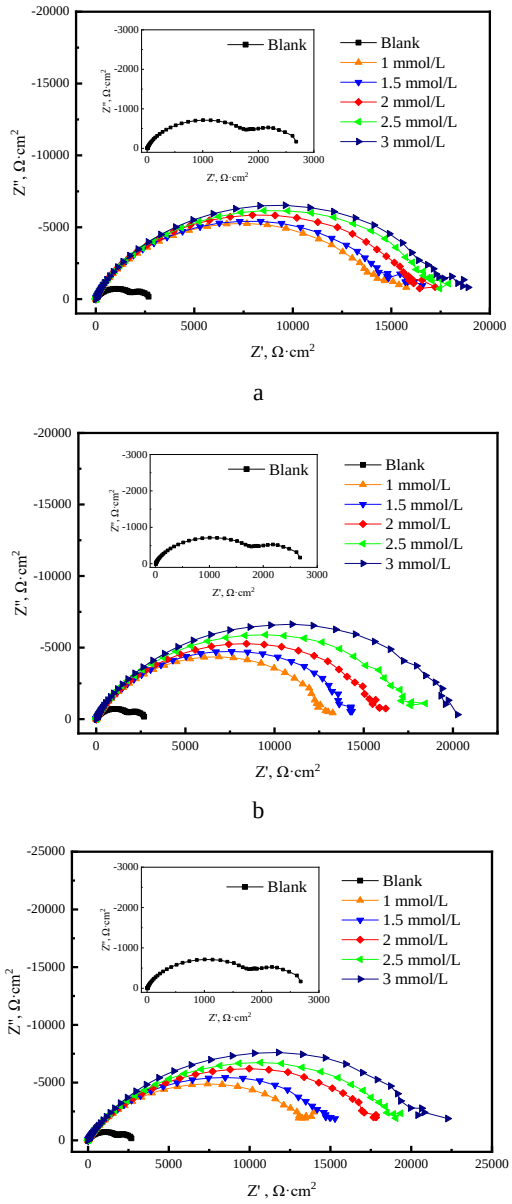

Fig. 2. Nyquist plots after adding various concentrations of three inhibitors: a – TAZ; b – ATA; c – DAT

As seen in the Nyquist plots, compared to the blank condition, the presence of TAZ, ATA, and DAT caused a significant increase in the capacitive loop diameter. With the increase of the concentration, the capacitive loops of TAZ, ATA, and DAT gradually increased, reaching the maximum at 3 mmol/L. This revealed that the three corrosion inhibitors adsorbed onto the HAl77-2 surface, hindered the substance and charge transfer at the interface, and effectively inhibited the corrosion processes. Moreover, the Nyquist pattern was a non-ideal semicircle due to the presence of dispersion effects, which were caused by the roughness and heterogeneity of the HAl77-2 surface.

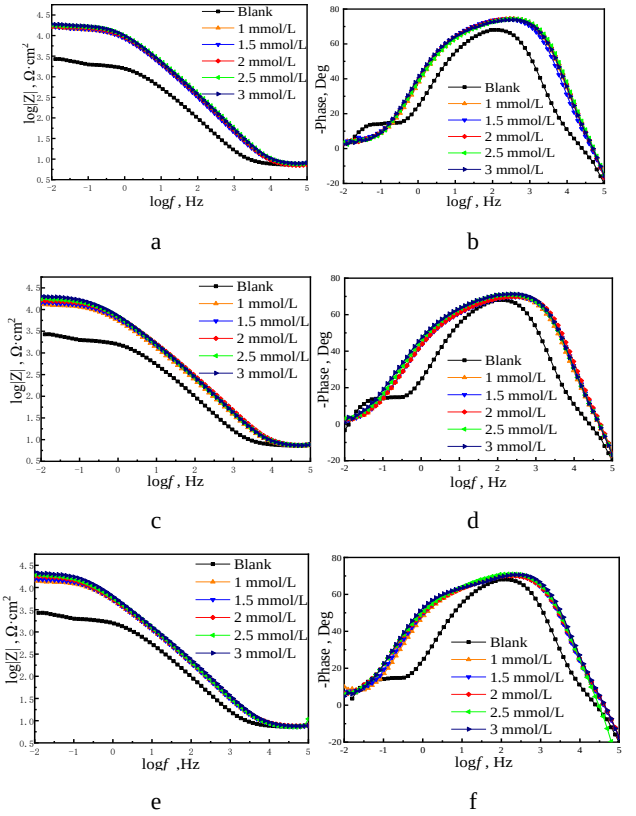

Fig. 3. Bode plots (phase angle/impedance modulus) after adding various concentrations of three inhibitors: a, b – TAZ; c, d – ATA; e, f – DAT

In the Bode plots, both the impedance modulus and phase angle also showed the same trend as that of the capacitive loop. Compared with the blank condition, the log|Z| values in the low- frequency region increased significantly, while the phase angle values shifted positively. This all indicated that TAZ, ATA, and TAZ were effectively adsorbed on the HAl77-2 surface with good corrosion inhibition performances. In addition, the wide phase angle values in the mid-frequency region speculate the presence of two time constants [5, 17]. The presence of two time constants indicates that the adsorption of TAZ, ATA, and DAT on the HAl77-2 surface produced two relaxation processes which were related to the double electrode layer capacitance and surface adsorption-desorption processes, respectively. In addition to this, inductive behavior appeared in the high-frequency region, i.e., the phase angle was below sub-zero degrees, which was caused by the internal resistance of the conductors resulting from the cable line connection [18].

The EIS plots were fitted through the equivalent circuit shown in Fig. 4 [18]. L is the inductance, representing the internal resistance of the wire, Rs is the solution resistance, CPEf and Rf are the capacitance and resistance of the outer layer film, respectively, CPEdl is the double electrode layer capacitance, and Rct is the charge transfer resistance.

Considering the inhomogeneity of the electrode surface, the constant phase element CPE is used in place of the ideal capacitance C. Its impedance value is defined as Eq. 2 [18]:

$$Z_{CPE} = \frac{1}{Y_0(jw)^n}, \quad (2)$$

where Y_0 is the constant phase angle element parameter, j is the imaginary root, n is the degree of dispersion, and w is the angular frequency.

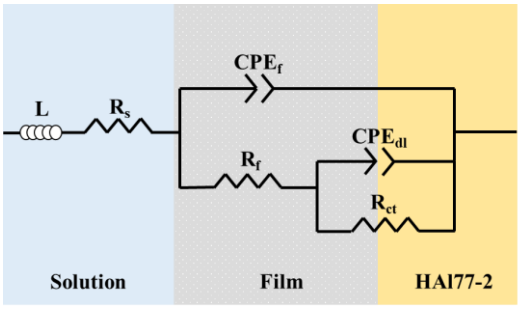

Fig. 3. Equivalent circuit for fitting [18]

The inhibition efficiency can be calculated using the following Eq. 3 [19]:

$$IE(\%) = \frac{R_p - R_{P,0}}{R_p} \times 100, \quad (3)$$

where R_p is the polarization resistance, which is equal to R_f + R_{ct}, and $R_{p,0}$ and R_p are the polarization resistances without and with inhibitor, respectively [19].

As shown in Table 3, the TAZ, ATA, and DAT resulted in significant increases in the Rct values. This indicated that these three corrosion inhibitors could effectively inhibit the charge transfer process of the HAl77-2 corrosion reactions in the 3.5 wt.% NaCl solutions, thus increasing the corrosion resistance and playing an inhibitory role. The maximum R_p values of TAZ, ATA, and DAT were reached at 3 mmol/L, when the corrosion inhibition efficiency was the largest. The corrosion inhibition efficiencies of the three corrosion inhibitors were relatively similar with values of 84.4 %, 86.4 %, and 87.1 %, respectively.

Compared with the blank condition, the film resistance Rf increased with the increasing concentration of the three corrosion inhibitors, and CPEf decreased, indicating that TAZ, ATA and DAT were effectively adsorbed onto the surface, and formed protective films that hindered the contact between Cl− ions and the HAl77-2 substrate. The double-layer capacitance CPEdl also decreased because of the adsorption of the three corrosion inhibitors at the metal/solution interface, which replaced the water molecules and adsorbed ions on the HAl77-2 surface, reducing the exposed areas and causing the double layer thickness to increase. This indicated that the effective adsorption processes of three corrosion inhibitors occurred on the HAl77-2 surface.

Table 3. Nyquist parameters after adding various concentrations of three inhibitors

Inhibitor	C, mmol/L	L, μH	R_s, Ω·cm^2	CPE_f, μF·cm^{-2}	n_f	R_f, Ω·cm^2	CPE_{dl}, μF·cm^{-2}	n_{dl}	R_{ct}, Ω·cm^2	R_p, Ω·cm^2	IE, %
	Blank	5.06	6.99	51.81	0.83	1843	2796	0.84	1021	2864	–
TAZ	1.0	4.54	7.24	7.74	0.90	1534	13.48	0.65	13583	15117	81.1
	1.5	4.73	7.60	8.62	0.90	1525	14.35	0.63	14224	15749	81.8
	2.0	4.53	6.79	7.38	0.91	1344	13.05	0.65	15570	16914	83.1
	2.5	4.60	7.33	6.34	0.91	1415	12.67	0.65	16479	17894	84.0
	3.0	4.76	7.60	6.95	0.91	1326	11.85	0.67	17071	18397	84.4
ATA	1.0	4.59	6.84	14.38	0.87	1063	25.07	0.64	12314	13377	78.6
	1.5	4.67	7.19	11.90	0.87	1057	24.29	0.63	13811	14868	80.7
	2.0	4.67	7.17	10.34	0.88	953	22.09	0.63	15681	16634	82.8
	2.5	4.67	7.13	12.46	0.87	1359	22.22	0.62	17253	18612	84.6
	3.0	4.69	7.11	11.19	0.88	1126	22.51	0.62	19941	21067	86.4
DAT	1.0	4.52	7.19	16.94	0.87	1061	27.69	0.64	13683	14744	80.6
	1.5	4.55	7.12	18.08	0.87	1313	26.95	0.65	14926	16239	82.4
	2.0	4.68	7.33	17.39	0.86	1518	28.49	0.63	17708	19226	85.1
	2.5	8.48	6.87	17.75	0.86	2080	26.00	0.65	18406	20486	86.0
	3.0	4.68	7.30	13.63	0.88	1191	23.28	0.68	21096	22287	87.1

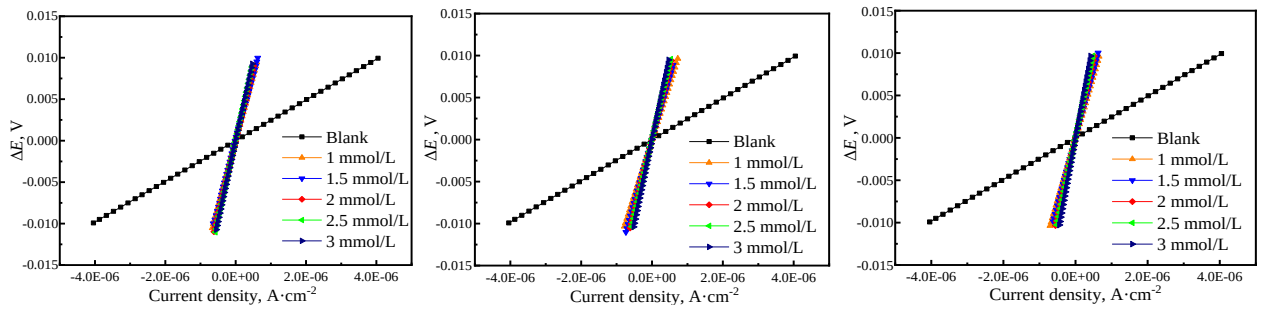

Fig. 4. Linear polarization resistance curves after adding various concentrations of three inhibitors: a – TAZ; b – ATA; c – DAT

3.3. Linear polarization resistance (LPR) tests

For coupled systems or alloys, there is an interactive polarization effect between metal elements, so linear polarization resistance (LPR) test is a suitable method for studying corrosion behavior and mechanism. To further evaluate the inhibition properties of the three corrosion inhibitors, LPR tests were performed, as shown in Fig.5. The slope of the curve reflects the magnitude of the polarization resistance (Rp). Compared with the sample in the blank solution, the slope increased with the addition of TAZ, ATA, and DAT. From the linear polarization resistance curves, these results agreed well with the EIS tests and further indicated that the TAZ, ATA and DAT had good inhibitory effects on the corrosion processes of HAl77-2.

The linear polarization parameters were obtained by fitting the LPR curves, and the inhibition efficiency was also calculated by Eq. 3. As shown in Table 4, the corrosion rate and corrosion current density were reduced by the addition of TAZ, ATA, and DAT, respectively. Meanwhile, the values of Rp increased, reaching maximum values of 19500 Ω·cm^2, 20179 Ω·cm^2 and 23062 Ω·cm^2 at 3 mmol/L, respectively. As the concentration increased, the number of corrosion inhibitor molecules increased, and the protective film that formed became denser, which hindered the corrosion reactions. In addition, the Ecorr values all moved in the negative direction, which indicated that the adsorption of the TAZ , ATA, and DAT on the HAl77-2 surface enhanced the cathodic polarization process and mainly inhibited the oxygen reduction process [20, 21]. Furthermore, the corrosion inhibition efficiencies of the ATA, and DAT were higher than those of the TAZ, with maximum values of 87.8 % (ATA), 89.4 % (DAT), and 87.4 % (TAZ). Thus, all three exhibited good corrosion inhibition performances.

3.4. Adsorption isotherm studies

The adsorption mechanisms of the TAZ, ATA and DAT on the HAl77-2 surface were inferred by developing an adsorption isotherm model. The surface coverage (θ) was obtained from the EIS data at 30 °C by the following Eq. 4 [20]:

$$\theta = IE/100. \quad (4)$$

Typical adsorption isotherms include Langmuir, Temkin, Freundlich, EI-Awady, etc [22]. In particular, the Langmuir adsorption isotherm had the highest linear correlation coefficient. Therefore, the Langmuir adsorption isotherm was considered the most suitable model. The model formula [22] can be represented as:

$$\frac{C}{\theta} = \frac{1}{K_{ads}} + C, \quad (5)$$

where C is the concentration, θ is the surface coverage, and K_{ads} is the adsorption equilibrium constant.

Fig. 6 shows plots with C as the horizontal coordinate and C/θ as the vertical coordinate. The R^2 values derived from the EIS tests were 0.9999, 0.9994 and 0.9998, respectively. These results indicated that C and C/θ had a highly linear relationship, and the adsorption processes of three corrosion inhibitors followed the Langmuir adsorption isotherm model, which suggests there is only one layer of adsorbed molecules at the solid/liquid interface, i.e., the TAZ, ATA, and DAT formed single-molecule adsorption films on the HAl77-2 surface, respectively, which inhibited the corrosion processes [23].

The intercept of the fitted curve is $1/K_{ads}$, and the adsorption free energy (ΔG_{ads}) was calculated as follows:

$$\Delta G_{ads} = -RTln55.5K_{ads}, \quad (6)$$

where R is the gas constant, with a value of 8.314 J/(K·mol), and T is the absolute temperature, with units of K. The results are summarized in Table 5.

Table 4. Thermodynamic parameters of three inhibitors on the HAl77-2 surface

Inhibitor	K_{ads}, L/mmol	ΔG_{ads}, kJ/mol
TAZ	11.34	−33.64
ATA	5.10	−31.62
DAT	6.37	−32.18

The values of K_{ads} were 11.34 L/mmol, 5.10 L/mmol and 6.37 L/mmol, respectively. The negative values of ΔGads indicate that the adsorption of the TAZ, ATA, and DAT on the HAl77-2 surface was spontaneous.

Table 5. Linear polarization resistance parameters after adding various concentrations of three inhibitors

Inhibitor	C, mmol/L	v, 10^{-3}mmPY	E_{corr}, V	i_{corr}, μA·cm^{-2}	R_p, Ω·cm^2	IE, %
	Blank	125.02	-0.246	10.629	2454	–
TAZ	1.0	19.388	-0.318	1.6484	15826	84.5
	1.5	19.209	-0.323	1.6331	15974	84.6
	2.0	17.278	-0.323	1.4689	17759	86.2
	2.5	16.004	-0.322	1.3606	19173	87.2
	3.0	15.735	-0.323	1.3378	19500	87.4
ATA	1.0	23.157	-0.323	1.9688	13250	81.5
	1.5	20.546	-0.326	1.7468	14934	83.6
	2.0	18.016	-0.326	1.5317	17032	85.6
	2.5	16.960	-0.330	1.4419	18092	86.4
	3.0	15.206	-0.333	1.2928	20179	87.8
DAT	1.0	20.804	-0.314	1.7687	14749	83.4
	1.5	19.176	-0.319	1.6303	16002	84.7
	2.0	16.526	-0.324	1.4050	18567	86.8
	2.5	15.485	-0.327	1.3165	19815	87.6
	3.0	13.305	-0.329	1.1312	23062	89.4

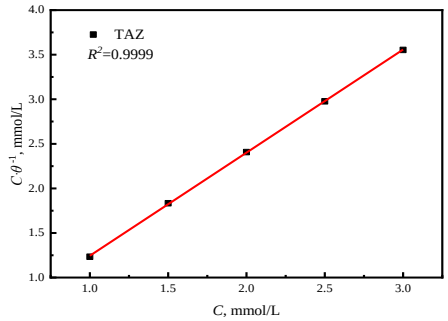

a

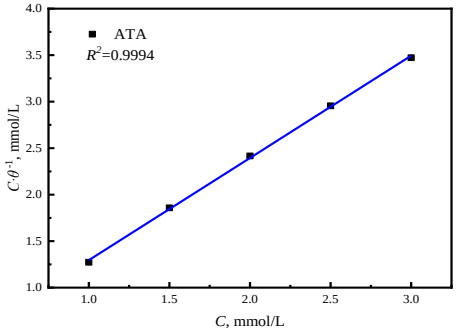

b

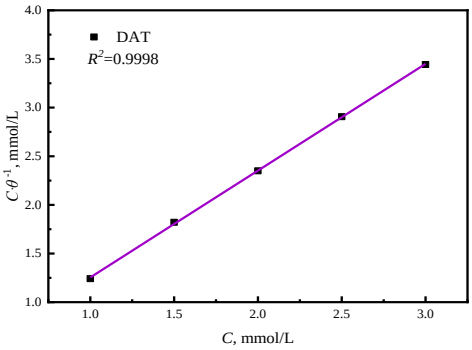

c

Fig. 6. Langmuir adsorption isotherms of three inhibitors: a – TAZ; b – ATA; c – DAT

The absolute value of ΔGads was considered to correspond to physisorption if it was lower than 20 kJ/mol. If it was between 20 and 40 kJ/mol, physisorption and chemisorption occurred together [24]. If the value was higher than 40 kJ/mol, the adsorption was considered to be chemisorption [25, 26]. According to ΔGads, the adsorption types of the three inhibitors on the HAl77-2 surface were mixed-type adsorption, i.e., both physisorption and chemisorption.

3.5. Surface characteristic analysis

Fig. 7 and Table 6 show SEM images and elemental compositions of HAl77-2 after 72 h exposure in a corrosion inhibitor-free solution. The surface morphologies of the HAl77-2 after 72 h of exposure to solutions free of and containing corrosion inhibitors were examined via SEM. In the blank solution, the HAl77-2 became rough due to erosion, and the surface was severely damaged, containing large amounts of corrosion products. However, smoother surfaces were obtained under the protection of the three corrosion inhibitors. It was clearly seen that the DAT and ATA showed better corrosion inhibition than TAZ, confirming the results of electrochemical tests. The three corrosion inhibitors effectively inhibited the erosion of the HAl77-2 by adsorption on its surface.

Table 6. Elemental compositions of the HAl77-2 without and with the presence of inhibitors

Elements, at%	Blank	TAZ	ATA	DAT
C	31.5	44.4	43.0	42.8
N	–	29.2	24.5	29.8
O	37.1	3.9	8.1	5.5
Cu	13.2	15.5	16.2	13.1
Zn	11.0	5.8	5.9	4.1
Cl	7.1	1.3	2.3	4.6

3.6. Theoretical computational studies

From the abovementioned experiments, the adsorption processes of the three corrosion inhibitors on the HAl77-2 surface were mixed-type adsorption, with charge sharing or transfer between the corrosion inhibitor molecules and HAl77-2 [29].

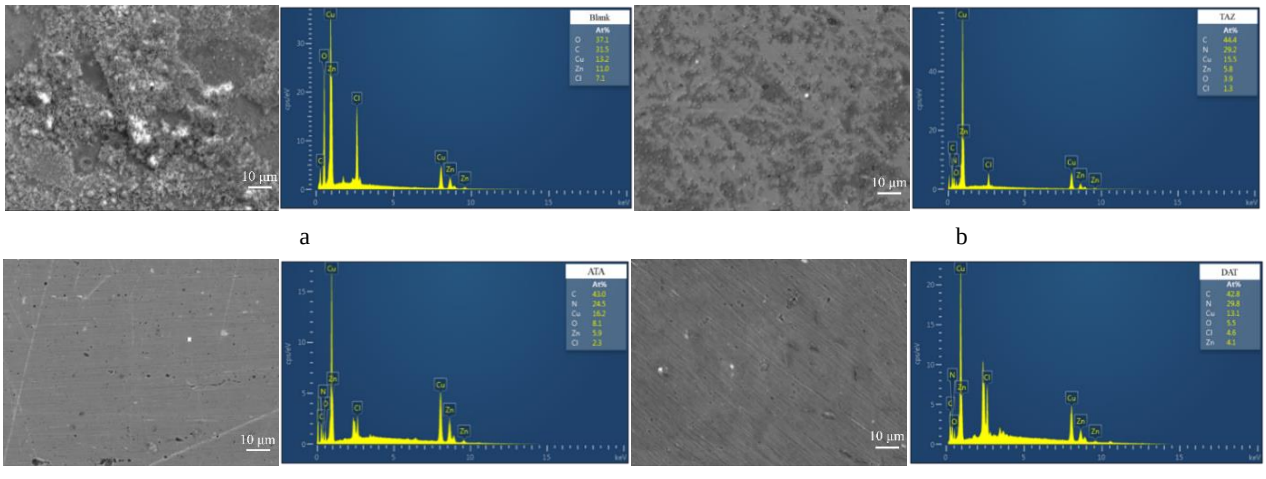

Fig. 7. SEM and EDS images of HAl77-2 without and with the presence of inhibitors: a – blank; b – TAZ; c – ATA; d – DAT

Quantum chemistry calculations are a powerful tool to study the adsorption mechanisms of organic molecules [29, 30]. Therefore, in this section, quantum chemistry calculations were used to investigate the adsorption mechanism of the TAZ, ATA, and DAT on the HAl77-2 surface.

The optimized molecules possessed near-planar structures. If the inhibitor molecule was close to a planar structure, it was more favorable for the active center to interact with the metal surface and thus inhibit corrosion. Thus, the TAZ, ATA, and DAT adsorbed in parallel on the HAl77-2 surface, thus providing protection.

The Mulliken charge distribution is one of the most commonly used methods to calculate the molecular charge density, and it can be used to analyze the active adsorption centers of corrosion inhibitors [3, 31]. The high charge density in the molecular structure favors the formation of adsorption centers [32]. As shown in Fig. 8, the N atoms were adsorption centers with high charge densities. The charge densities of N atoms on the $–NH_2$ group were higher than those on the five-membered ring.

Frontier molecular orbital theory suggests that the HOMO and LUMO molecular orbital distributions reflect the electron-donating and electron-receiving abilities of the inhibitor, respectively. The uniform distributions of the HOMO and LUMO orbitals of TAZ and ATA suggested that the entire molecule could either donate electrons to the empty orbitals of HAl77-2 to form coordination bonds or receive free electrons to form feedback bonds that adsorbed onto the HAl77-2 surface. For DAT, the HOMO orbital was distributed over the whole molecular structure, while the LUMO orbital was mainly distributed near the N6 atom, which was consistent with Lei Guo's calculation.

Table 7 shows the quantum chemistry parameters of the three corrosion inhibitors, and the corrosion inhibition efficiency was taken from the EIS tests. EHOMO represents the electron-donating ability of the corrosion inhibitor molecule. The higher the value, the more unstable the electrons in the orbital, and the more easily the molecule can donate electrons to the empty orbital of the metal.

The lower the value of ELUMO, the easier it is for the molecule to receive electrons [33]. ΔE is the energy gap between the two orbitals, which reflects the stability of the corrosion inhibitor molecule. The smaller the value, the lower the stability of the molecule, and the more favorable it is to bond with the metal [34]. In general, the inhibition efficiency of corrosion inhibitors increases with the increase of EHOMO and the decrease of Δ*E*. In Table 7, the order of EHOMO was (−5.448 eV) > ATA (−6.033 eV) > TAZ (−7.796 eV), and the order of ΔE was DAT (5.022 eV) < ATA (5.969 eV) < TAZ (7.351 eV), which was consistent with the experimental results. The lower the total energy of the molecule, the more active the molecule is, the higher the corrosion inhibition efficiency. The order of total energy values was DAT (−9607.66 eV) < ATA (−8100.71 eV) < TAZ (−6593.77eV), indicating that DAT was the most active and had the strongest corrosion inhibition performance.

Other parameters were calculated by the following equations [35]:

$$\chi = (I + A)/2; \quad (7)$$

$$\eta = (I - A)/2; \quad (8)$$

$$\sigma = \eta^{-1}; \quad (9)$$

$$I = -E_{\mathrm{HOMO}}; \quad (10)$$

$$A = -E_{\mathrm{LUMO}}, \quad (11)$$

where χ is the absolute electronegativity, η is the global hardness, σ is the global softness, I and A are the ionization potential and electron affinity potential, respectively.

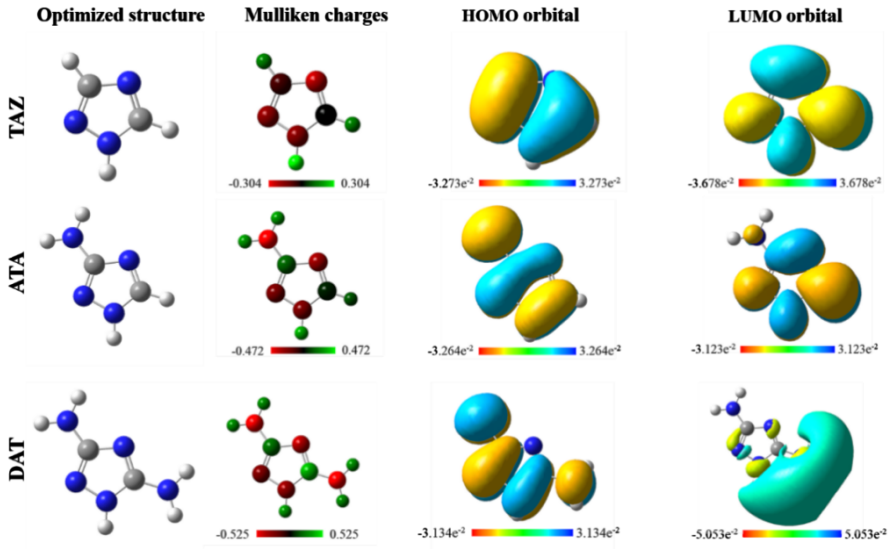

Fig. 8. Optimized structures, Mulliken charges and Frontier molecular orbital density distributions of three inhibitors

Table 7. Quantum chemistry parameters of three inhibitors

Inhibitor	E_{HOMO}, eV	E_{LUMO}, eV	Δ*E*, eV	Total energy, eV	μ (Debye)	*IE*, %
TAZ	–7.796	–0.445	7.351	–6593.77	2.9262	84.4
ATA	–6.033	–0.064	5.969	–8100.71	1.3301	86.4
DAT	–5.448	–0.426	5.022	–9607.66	2.8044	87.1

In general, the lower the electronegativity (χ) value, the higher the electron-donating tendency of the corrosion inhibitor molecule. Table 8. shows the Global active parameters of three inhibitors, the order of the electronegativity (χ) was DAT (2.937 eV) < ATA (3.049 eV) < TAZ (4.121 eV), indicating the better electron-donating ability of the DAT.

Table 8. Global active parameters of three inhibitors

Inhibitor	*I*, eV	*A*, eV	χ, eV	η, eV	σ, eV
TAZ	7.796	0.445	4.121	3.676	0.272
ATA	6.033	0.064	3.049	2.985	0.335
DAT	5.448	0.426	2.937	2.511	0.398

The global hardness (η) and softness (σ) represent the stability and activity of the corrosion inhibitor molecule. Compared with the TAZ, the DAT and ATA showed lower η (2.511 eV, 2.985 eV) and higher σ (0.398 eV, 0.335 eV), indicating that they were more reactive. The results of the abovementioned quantum chemistry parameters were consistent with the corrosion inhibition efficiency, and the DAT had a better corrosion inhibition ability.

3.7. Corrosion inhibition mechanism studies

HAl77-2 contains a certain content of Al, which can form a protective oxide film on the surface of the alloy, which can hinder the diffusion and migration of ions in the lattice when corrosion occurs, so the corrosion resistance and resistance to dezincification corrosion are improved compared with brass. However, in the harsh Cl– environment, after a long period of erosion, uniform corrosion and dezincification corrosion are equally inevitable.

From the above tests, the presence of the three corrosion inhibitors resulted in good protection of the HAl77-2 sample surface, reduced the amounts of corrosion products, and inhibited the dezincification corrosion of the alloy. This is attributed to the mixed adsorption processes of the three corrosion inhibitors on the surface, Fig. 9 shows the Diagram of the adsorption mechanism of the three inhibitors.

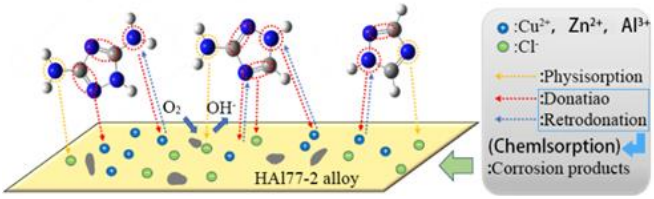

Fig. 9. Diagram of adsorption mechanism of three inhibitors

First, the activated dissolution of HAl77-2 metallic elements resulted in a positively charged surface, which attracted the negatively charged Cl– adsorbed onto the sample surface. The –NH2 and N atoms in the molecular structure of the three corrosion inhibitors adsorbed to the HAl77-2 surface due to the electrostatic interaction with Cl–, retarding the corrosion of the matrix, i.e., the physisorption. Second, the TAZ, ATA, and DAT formed coordination bonds mainly by interacting with the HAl77-2 empty orbitals through lone-electron pairs on the N atoms and π-electrons on the TAZ ring, while accepting free electrons to form feedback bonds. The three corrosion inhibitors adsorbed to the HAl77-2 surface in parallel by forming donor-acceptor interactions, effectively inhibiting the corrosion of HAl77-2 in Cl– media, i.e., the chemisorption.

4. CONCLUSIONS

In this paper, the corrosion inhibition properties and mechanism of 1,2,4-triazole (TAZ) and its derivatives 3-amino-1,2,4-triazole (ATA) and 3,5-diamino-1,2,4-triazole (DAT) in 3.5 wt.% NaCl solutions for HAl77-2 aluminum brass were investigated, and the specific conclusions are as follows.

1. The results of weight loss tests and EIS tests showed that all three corrosion inhibitors exhibited good inhibition performances. The results showed that TAZ, ATA and DAT effectively inhibited the corrosion of HAl77-2. The maximum inhibition efficiencies of the three corrosion inhibitors were 84.4 %, 86.4 %, and 87.1 %, respectively. The LPR tests results showed that the three corrosion inhibitors mainly inhibited the cathodic oxygen reduction process, effectively reducing the corrosion rate and current density.
2. The adsorption behavior of the TAZ, ATA, and DAT on the HAl77-2 surface followed the Langmuir adsorption isotherm model, and all were mixed adsorption processes (including both physisorption and chemisorption).
3. SEM and EDS analysis showed that smoother surfaces were obtained in the presence of the three corrosion inhibitors, respectively. The presence of N and the increase in the ratio of C confirmed the adsorption of TAZ, ATA and DAT on the HAl77-2 surface.
4. Quantum chemistry calculation results showed that the three corrosion inhibitors had good electron-donating abilities and exerted corrosion inhibition effects by parallel adsorption to form a film on the HAl77-2 surface with N atoms as the active adsorption centers. The calculated parameters were consistent with the test results.

Acknowledgments

This study was funded by the National Natural Science Foundation of China (NSFC, No. 52171092). We thank LetPub (www.letpub.com) for its linguistic assistance during the preparation of this manuscript.

REFERENCES

1. **Lei, Y., Ohtsuka, T., Sheng, N.** Corrosion Protection of Copper by Polypyrrole Film Studied by Electrochemical Impedance Spectroscopy and the Electrochemical Quartz Microbalance *Applied Surface Science* 357 (Part A) 2015: pp. 1122 – 1132. http://doi.org/10.1016/j.apsusc.2015.09.053
2. **Fateh, A., Aliofkhazraei, M., Rezvanian, A.R.** Review of Corrosive Environments for Copper and Its Corrosion Inhibitors *Arabian Journal of Chemistry* 13 (1) 2020: pp. 481 – 544. http://doi.org/10.1016/j.arabjc.2017.05.021
3. **El-Katori, E.E., Ahmed, M., Nady, H.** Imidazole Derivatives Based on Glycourils as Efficient Anti-corrosion Inhibitors for Copper in HNO_3 Solution: Synthesis,

Electrochemical, Surface, and Theoretical Approaches *Colloids and Surfaces A: Physicochemical and Engineering Aspects* 649 2022: pp. 129391. http://doi.org/10.1016/j.colsurfa.2022.129391

4. **Mo, Y., Jiang, Y., Liu, X., Xie, J.** Effects of Microstructure on the Deformation Behavior, Mechanical Properties and Residual Stress of Cold-rolled HAl77-2 Aluminum Brass Tube *Journal of Materials Processing Technology* 235 2016: pp. 75 – 84. http://doi.org/10.1016/j.jmatprotec.2016.04.016
5. **Yu, Y., Yang, D., Zhang, D., Wang, Y., Gao, L.** Anti-corrosion Film Formed on HAl77-2 Copper Alloy Surface by Aliphatic Polyamine in 3 wt.% NaCl Solution *Applied Surface Science* 392 (1) 2017: pp. 768 – 776. http://doi.org/10.1016/j.apsusc.2016.09.118
6. **Quraishi, M.A., Chauhan, D.S., Saji, V.S.** Heterocyclic Biomolecules as Green Corrosion Inhibitors *Journal of Molecular Liquids* 341 (Suppl C) 2021: pp. 117265. http://doi.org/10.1016/j.molliq.2021.117265
7. **Wang, Q., Zhang, Q., Liu, L., Zheng, H., Wu, X., Li, Z., Gao, P., Sun, Y., Yan, Z., Li, X.** Experimental, DFT and MD Evaluation of Nandina Domestica Thunb. Extract as Green Inhibitor for Carbon Steel Corrosion in Acidic Medium *Journal of Molecular Structure* 1265 2022: pp. 133367. http://doi.org/10.1016/j.molstruc.2022.133367
8. **Ou, H.H., Tran, Q.T.P., Lin, P.H.** A Synergistic Effect Between Gluconate and Molybdate on Corrosion Inhibition of Recirculating Cooling Water Systems *Corrosion Science* 133 2018: pp. 231 – 239. http://doi.org/10.1016/j.corsci.2018.01.014
9. **Zhang, Q.H., Hou, B.S., Li, Y.Y., Lei, Y., Wang, X., Liu, H.F., Zhang, G.A.** Two Amino Acid Derivatives as High Efficient Green Inhibitors for the Corrosion of Carbon Steel in CO_2-saturated Formation Water *Corrosion Science* 189 (Suppl C) 2021: pp. 109596. http://doi.org/10.1016/j.corsci.2021.109596
10. **Gutiérrez, E., Rodríguez, J.A., Cruz-Borbolla, J., Alvarado-Rodríguez, J.G., Thangarasu, P.** Development of a Predictive Model for Corrosion Inhibition of Carbon Steel by Imidazole and Benzimidazole Derivatives *Corrosion Science* 108 2016: pp. 23 – 35. http://doi.org/10.1016/j.corsci.2016.02.036
11. **Kesari, P., Udayabhanu, G.** Investigation of Vitamin B12 as a Corrosion Inhibitor for Mild steel in HCl Solution Through Gravimetric and Electrochemical Studies *Ain Shams Engineering Journal* 14 (4) 2022: pp. 101920. http://doi.org/10.1016/j.asej.2022.101920
12. **Sabet Bokati, K., Dehghanian, C.** Adsorption Behavior of 1H-benzotriazole Corrosion Inhibitor on Aluminum Alloy 1050, Mild Steel and Copper in Artificial Seawater *Journal of Environmental Chemical Engineering* 6 (2) 2018: pp. 1613 – 1624. http://doi.org/10.1016/j.jece.2018.02.015
13. **Yin, D., Yang, L., Tan, B., Ma, T., Zhang, S., Wang, Y., Guo, L., Gao, B., He, Y.** Theoretical and Electrochemical Analysis on Inhibition Effects of Benzotriazole Derivatives (un- and methyl) on Copper Surface *Journal of Molecular Structure* 1243 2021: pp. 130871. http://doi.org/10.1016/j.molstruc.2021.130871
14. **Albini, M., Letardi, P., Mathys, L., Brambilla, L., Schröter, J., Junier, P., Joseph, E.** Comparison of a Bio-based Corrosion Inhibitor Versus Benzotriazole on Corroded Copper Surfaces *Corrosion Science* 143 2018: pp. 84 – 92. http://doi.org/10.1016/j.corsci.2018.08.020
15. **Li, W., Tan, B., Zhang, S., Guo, L., Ji, J., Yan, M., Wang, R.** Insights into Triazole Derivatives as Potential Corrosion Inhibitors in CMP Process: Experimental Evaluation and Theoretical Analysis *Applied Surface Science* 602 2022: pp. 154165. http://doi.org/10.1016/j.apsusc.2022.154165
16. **El Ibrahimi, B., Soumoue, A., Jmiai, A., Bourzi, H., Oukhrib, R., El Mouaden, K., El Issami, S., Bazzi, L.** Computational Study of Some Triazole Derivatives (Un- and Protonated Forms) and Their Copper Complexes in Corrosion Inhibition Process *Journal of Molecular Structure* 1125 2016: pp. 93 – 102. http://doi.org/10.1016/j.molstruc.2016.06.057
17. **Zeng, Y., Kang, L., Wu, Y., Wan, S., Liao, B., Li, N., Guo, X.** Melamine Modified Carbon Dots as High Effective Corrosion Inhibitor for Q235 Carbon Steel in Neutral 3.5 wt.% NaCl Solution *Journal of Molecular Liquids* 349 2022: pp. 118108. http://doi.org/10.1016/j.molliq.2021.118108
18. **Padhan, S., Rout, T.K., Nair, U.G.** N-doped and Cu,N-doped Carbon Dots as Corrosion Inhibitor for Mild Steel Corrosion in Acid Medium *Colloids and Surfaces A: Physicochemical and Engineering Aspects* 653 2022: pp. 129905. http://doi.org/10.1016/j.colsurfa.2022.129905
19. **Zhang, Y., Zhang, S., Tan, B., Guo, L., Li, H.** Solvothermal Synthesis of Functionalized Carbon Dots from Amino Acid as an Eco-friendly Corrosion Inhibitor for Copper in Sulfuric Acid Solution *Journal of Colloid and Interface Science* 604 2021: pp. 1 – 14. http://doi.org/10.1016/j.jcis.2021.07.034
20. **Shao, H., Yin, X., Zhang, K., Yang, W., Chen, Y., Liu, Y.** N-[2-(3-indolyl)ethyl]-cinnamamide Synthesized from Cinnamomum Cassia Presl and Alkaloid Tryptamine as Green Corrosion Inhibitor for Q235 Steel in Acidic Medium *Journal of Materials Research and Technology* 20 2022: pp. 916 – 933. http://doi.org/10.1016/j.jmrt.2022.07.122
21. **Zhang, Q.H., Hou, B.S., Li, Y.Y., Zhu, G.Y., Liu, H.F., Zhang, G.A.** Two Novel Chitosan Derivatives as High Efficient Eco-friendly Inhibitors for the Corrosion of Mild Steel in Acidic Solution *Corrosion Science* 164 2020: pp. 108346. http://doi.org/10.1016/j.corsci.2019.108346
22. **Zhang, K., Yang, W., Xu, B., Chen, Y., Yin, X., Liu, Y., Zuo, H.** Inhibitory Effect of Konjac Glucomanan on Pitting Corrosion of AA5052 Aluminium Alloy in NaCl Solution *Journal of Colloid and Interface Science* 517 2018: pp. 52 – 60. http://doi.org/10.1016/j.jcis.2018.01.092
23. **Huan, Y., Dai, S., Liu, P., Zhu, Y.** Synergistic Mechanism of Ternary Green Corrosion Inhibitors for N80 Steel in 20 wt.% HCl Solution: Encapsulation and Transportation of Vanillin Through Micelles Formed by Ionic Liquids *Corrosion Science* 227 2024: pp. 111750. http://doi.org/10.1016/j.corsci.2023.111750
24. **Gao, L., Peng, S., Huang, X., Gong, Z.** A Combined Experimental and Theoretical Study of Papain as a Biological Eco-friendly Inhibitor for Copper Corrosion in H_2SO_4 Medium *Applied Surface Science* 511 2020: pp. 145446. http://doi.org/10.1016/j.apsusc.2020.145446
25. **Wang, X., Guo, H., Cai, S., Xu, X.** Expired Antihypertensive Drugs as Eco-friendly and Efficient

Corrosion Inhibitors for Carbon Steel in CO_2-saturated Oilfield Water: Experimental and Theoretical Approaches *Journal of Molecular Structure* 1294 (Part 1) 2023: pp. 136555. http://doi.org/10.1016/j.molstruc.2023.136555

26. **Wang, J., Wang, Y., Yang, Z., Guo, L., Yang. J., Yang, Q., Wu, J.** Synthesis of a Novel Fused Heterocyclic Quaternary Ammonium Salt and its Performance in Ultra-low Dosage as Acidizing Corrosion Inhibitor *Journal of Molecular Structure* 1303 2024: pp. 137571. http://doi.org/10.1016/j.molstruc.2024.137571
27. **Lin, G., Zhou, Y., Zeng, J., Zou, Y., Liu, J., Sun, L.** Influence of Rare Earth Elements on Corrosion Behavior of Al-brass in Marine Water *Journal of Rare Earths* 29 (7) 2011: pp. 638 – 644. http://doi.org/10.1016/s1002-0721(10)60513-3
28. **Rao, T.S., Bera, S.** Protective Layer Dissolution by Chlorine and Corrosion of Aluminum Brass Condenser Tubes of a Nuclear Power Plant *Engineering Failure Analysis* 123 2021: pp. 105307. http://doi.org/10.1016/j.engfailanal.2021.105307
29. **Ju, H., Kai, Z.P., Li, Y.** Aminic Nitrogen-bearing Polydentate Schiff Base Compounds as Corrosion Inhibitors for Iron in Acidic Media: A Quantum Chemical Calculation *Corrosion Science* 50 (3) 2008: pp. 865 – 871. http://doi.org/10.1016/j.corsci.2007.10.009
30. **Hanane, H., Tahar, D., Moursa, A.N., Saifi, I., Djamel, D., Salah, C.** Electrochemical and Quantum Chemical Studies of Some Azomethine Compounds as Corrosion Inhibitors for Mild Steel in 1M Hydrochloric Acid *Corrosion Science* 88 (14) 2014: pp. 234 – 245. http://doi.org/10.1016/j.corsci.2014.07.044
31. **Damej, M., Hsissou, R., Berisha, A., Azgaou, K., Sadiku, M., Benmessaoud, M., Labjar, N., El hajjaji, S.** New Epoxy Resin as a Corrosion Inhibitor for the Protection of Carbon Steel C38 in 1M HCl. Experimental and Theoretical Studies (DFT, MC, and MD) *Journal of Molecular Structure* 1254 2022: pp. 132425. http://doi.org/10.1016/j.molstruc.2022.132425
32. **Mashuga, M.E., Olasunkanmi, L.O., Lgaz, H., Sherif, E.S.M., Ebenso, E.E.** Aminomethylpyridazine Isomers as Corrosion Inhibitors for Mild Steel in 1 M HCl: Electrochemical, DFT and Monte Carlo Simulation Studies *Journal of Molecular Liquids* 344 2021: pp. 117882. http://doi.org/10.1016/j.molliq.2021.117882
33. **Wang, D.Y., Li, Z.G., Liu, Y., Li, H.J., Wu, Y.C.** Investigation of Efficient Corrosion Inhibitor During Acid Cleaning of Reverse Osmosis (RO) Desalination Plant *Corrosion Science* 208 2022: pp. 110609. http://doi.org/10.1016/j.corsci.2022.110609
34. **Singh, R., Prasad, D., Safi, Z., Wazzan, N., Guo, L.** De-scaling, Experimental, DFT, and MD-simulation Studies of Unwanted Growing Plant as Natural Corrosion Inhibitor for SS-410 in Acid Medium *Colloids and Surfaces A: Physicochemical and Engineering Aspects* A 649 2022: pp. 129333. http://doi.org/10.1016/j.colsurfa.2022.129333
35. **Ma, L., Lu, W., Yang, D., Shen, J., Gao, Z., Zhang, S., Liao, Q.** Dithiocarbamate Modified Glucose as a Novel Eco-friendly Corrosion Inhibitor for Copper in Sodium Chloride Media *Sustainable Chemistry and Pharmacy* 22 2021: pp. 100488. http://doi.org/10.1016/j.scp.2021.100488